IEEE Access
Multidisciplinary | Rapid Review | Open Access Journal

Received 11 December 2024, accepted 24 December 2024, date of publication 3 January 2025, date of current version 13 January 2025.

Digital Object Identifier 10.1109/ACCESS.2025.3525975

RESEARCH ARTICLE

A Timer and Mixed Integer Linear Programming Load Shedding Scheme for Resilient DC Microgrids

ABDULRAHMAN BABAGANA, (Student Member, IEEE), ISAH A. JIMOH, (Student Member, IEEE), YLJON SEFERI, AND GRAEME BURT, (Member, IEEE)
Institute for Energy and Environment, University of Strathclyde, G1 1XW Glasgow, U.K.

Corresponding author: Abdulrahman Babagana (abdulrahman.babagana@strath.ac.uk)

This work was supported by the Petroleum Trust Development Fund of Nigeria.

ABSTRACT Islanded DC microgrids are vulnerable to voltage instability caused by excessive power demand, which can adversely impact downstream consumers and disrupt overall microgrid operation. Existing load-shedding techniques face limitations such as over-shedding due to fixed voltage thresholds and time delays, predetermined load-shedding actions that fail to account for disturbance magnitude, and delayed stabilization caused by sequential load-shedding steps. To address these challenges, this paper proposes a novel load-shedding strategy for islanded DC microgrids that integrates a short-timer mechanism with Mixed Integer Linear Programming (MILP) optimization. The proposed approach reduces reliance on communication systems and achieves optimal load-shedding decisions using local voltage measurements. Simulation results on a DC microgrid model adapted from the IEEE 37-bus network demonstrate the effectiveness of the proposed scheme. The scheme results in a 20% reduction in unnecessary load shedding, an 18% improvement in voltage stabilization (measured as the final voltage after a disturbance), and a 25% decrease in response time compared to conventional methods. The results show that the proposed strategy ensures that the DC bus voltage remains above the critical threshold of 720 V, enhancing system reliability by minimizing voltage transients, reducing regulation time, and maintaining power balance. These improvements highlight the potential of the proposed scheme to support robust, secure, and resilient DC microgrid operation.

INDEX TERMS DC microgrid, distributed energy resources, load shedding, mixed-integer linear programming, optimization, resilience.

I. INTRODUCTION

Direct current (DC) microgrids have gained significant popularity globally due to their distinct advantages over traditional alternating current (AC) systems, particularly in regions like Africa and America [1], [2]. In sub-Saharan Africa, where over 50% of rural areas lacked grid access as of 2022, due to the high cost of transmission and distribution rendering centralised power solutions impractical [3], [4]. In contrast, in America, microgrids are critical in enhancing community resilience, particularly against extreme weather conditions, by ensuring a stable and reliable power supply [5]. DC microgrids provide a viable alternative for electrifying these underserved regions [5]. The growing adoption of DC microgrids can also be attributed to advancements in power electronics and the increasing demand for energy-efficient solutions. Most distributed energy resources (DERs), such as photovoltaic (PV) systems, fuel cells, and battery energy storage systems (BESSs), inherently generate DC power. Simultaneously, emerging loads like electric vehicles (EVs), consumer electronics, and LED lighting systems are predominantly DC-powered [2], [6]. Compared to their AC counterparts, DC microgrids offer several advantages, including the elimination of frequency,

The associate editor coordinating the review of this manuscript and approving it for publication was Arturo Conde.

phase, and reactive power controllers; lower capital costs and energy conversion losses due to reduced converter stages and the absence of AC/DC conversions; and enhanced immunity and resilience to disturbances originating from the utility grid [7]. However, key challenges remain, particularly in minimising voltage variations and ensuring proper current sharing among converters to mitigate disturbances and ensure system stability [8].

Voltage regulation and control challenges in DC microgrids have been extensively studied in [9], [10], and [11]. A key issue with control systems is their inability to maintain power balance during significant disturbances, particularly in islanded mode, where the DERs may not adequately regulate DC bus voltages. In such scenarios, a load-shedding scheme becomes essential to prevent voltage collapse and ensure critical loads receive reliable power. However, if the load-shedding scheme does not disconnect the appropriate loads promptly, the DC microgrid risks becoming unstable [12]. Additionally, unnecessary load shedding can reduce system reliability, underscoring the need for a precise and timely response.

Existing DC microgrid load-shedding schemes can be broadly categorized into communication-based and non-communication-based schemes based on their control method [13]. Communication-based schemes can collect and process microgrid data efficiently and timely. As a result, these load-shedding schemes are complex, costly, and vulnerable to communication failures. They also suffer from low flexibility, modality, and extendability [14], [15]. Due to these disadvantages, communication-based methods are typically suitable mostly for small-scale microgrids that do not require complex communication networks.

The non-communication-based schemes operate based on locally measured voltage signals [16]. Simplicity, cost-effectiveness, scalability, expandability, and robustness against communication failures are some of the advantages of this scheme. These schemes are, therefore, highly suitable for all DC microgrids, including those with geographically dispersed loads [17]. Further categorization of non-communication-based load-shedding approaches with conventional and adaptive schemes has been reported.

Conventional schemes consist of voltage-based, timer-based, and combined-based schemes. In contrast, adaptive schemes include adaptive voltage and adaptive timer-based schemes. The application of these schemes to DC microgrids has been extensively investigated. The voltage-based load shedding scheme [18], [19], [20] utilises different voltage thresholds to prioritise the shedding of non-critical loads. This method instantaneously sheds some load whenever its bus voltage exceeds the corresponding voltage threshold. The voltage-based scheme progressively sheds loads in steps. However, the scheme can cause unnecessary load shedding with large voltage deviations when the difference between the voltage thresholds is large. Thus, power supply reliability and bus voltage regulation performance must be traded off in this scheme.

The conventional timer-based strategy [20], [21] prioritizes non-critical loads and sheds them whenever their voltage falls below a common threshold for some time larger than the expected preset time delay. The process involves disconnecting non-critical loads in a predetermined order, using specific time delays for each load. The timer scheme comprises short and long delays with different time settings. However, there are a few downsides to this scheme. For instance, short delays can lead to over-shedding, and large delays can result in significant voltage sags. As a result, using a timer-based scheme can compromise power supply reliability and bus voltage regulation.

A combined scheme is reported in [20], [22] utilizing both timer-based and voltage-based algorithms and thus operating whenever one of the conditions for load shedding is satisfied. This scheme enjoys the merits of both voltage and timer-based schemes. However, the combined scheme is more likely to cause unnecessary load shedding due to the combination of predetermined voltage thresholds and time delays.

The adaptive voltage-based load-shedding scheme, as described in references [20], [23], adjusts voltage thresholds based on the ROCOV measured locally. This technique ensures quick and reliable load-shedding. However, it may cause low voltage and negatively affect critical loads, as lower voltage thresholds shed loads with lower priorities. Therefore, it is best suited for microgrids with few load-shedding steps. If many load-shedding steps need to be coordinated, the final step may occur at a significantly lower voltage. In such cases, using the strategy proposed in reference [24] for microgrids with a relatively small number of load-shedding steps is recommended.

The adaptive timer-based load-shedding scheme [20], [25] uses automatically adjusted time delays to coordinate the load-shedding. This scheme sheds non-critical loads using a time delay that adapts to the locally measured ROCOV and a common voltage threshold [25]. This scheme prevents unnecessary shedding of loads when ROCOV is insignificant and performs better than the adaptive voltage-based scheme regarding time regulation. However, similar to the adaptive voltage-based strategy [23] and timer-based scheme [21], the adaptive timer-based strategy utilizes a lower threshold, thereby exposing the critical loads to lower voltages.

A comprehensive comparison of existing non-communication-based load-shedding schemes for islanded DC microgrids was conducted in [20]. These schemes rely on fixed voltage thresholds, time delays, or ROCOV. However, they face significant limitations, including excessive bus voltage deviations, over-shedding of loads, and predetermined load-shedding actions that do not account for the magnitude of the disturbance. Additionally, these methods pose a risk of exposing critical loads to voltage instability during large disturbances and struggle to address voltage drops across long

distribution lines. These challenges underscore the need for more advanced load-shedding strategies that prioritize speed, optimal shedding, and system reliability.

Several optimisation techniques have been proposed to enhance load-shedding schemes in communication-based AC and DC networks. These methods are more accurate than traditional strategies in predicting power imbalances, providing improved load-shedding solutions, and are adaptive in reducing computational time. [26], [27]. Common techniques include artificial neural networks (ANN) [28], fuzzy logic control (FLC) [29], genetic algorithms (GA) [30], [31] and particle swarm optimization [30] are some of the commonly used methods to achieve this.

This paper introduces a novel timer-based Mixed Integer Linear Programming (MILP) load-shedding scheme for DC microgrids, designed to overcome the limitations of existing strategies and enhance system performance. The proposed approach employs a short-delay timer to trigger rapid load-shedding actions when a disturbance exceeds a predefined threshold. By integrating the MILP optimization algorithm, the scheme determines the optimal amount of non-critical loads to shed. The MILP algorithm assesses power imbalances and initiates load-shedding actions based on the severity of the disturbance, ensuring precise and efficient load management. This combined approach enables faster and more coordinated load-shedding actions, minimizing voltage deviations, preventing unnecessary disconnections, prioritizing critical loads, and maintaining overall microgrid stability. As a result, the proposed scheme addresses key limitations of existing adaptive and conventional methods, such as over-shedding, delayed response, and inefficiency in handling large disturbances. The key benefits of this approach are as follows:

- protects DC microgrid voltage stability and integrity by maintaining power balance under large disturbances,
- enables optimal shedding in large networks with many circuit breakers, i.e., sheds the best combination of non-critical loads without predefined order.
- prevents exposure of critical loads to excessive steady-state under-voltage conditions by avoiding under-shedding.
- operates effectively with short-time delays, thus avoiding over-shedding of non-critical loads associated with conventional short-time delays.

The remainder of this paper is organized as follows: Section II introduces the novel load-shedding scheme. Section III outlines the DC microgrid model used to implement and test the proposed strategy. Section IV presents a detailed discussion of the simulation results. Finally, V provides the conclusion of the study.

II. PROPOSED TIMER-BASED MIXED INTEGER LINEAR PROGRAMMING (MILP) LOAD SHEDDING SCHEME

The proposed timer-based mixed integer linear programming load-shedding scheme, also known as the MILP Timer-Based Load-Shedding Scheme, integrates a timer threshold to trigger load-shedding actions and employs an MILP algorithm to determine the optimal amount of non-critical load to shed. The scheme operates by shedding non-critical loads when the voltage measured at the load remains below a predefined threshold Vth set at 720 V, for a specified duration T_d. Each circuit breaker (CB) is assigned a time delay T_d, with an initial delay of 20 ms for the first and 10 ms for subsequent triggers. This design ensures rapid response to disturbances while maintaining system stability and preventing unnecessary load shedding.

A. ROLE OF MILP IN THE LOAD SHEDDING SCHEME

The MILP approach is employed here to solve the optimisation problem, determining the optimal amount of non-critical load to shed. Unlike traditional linear programming techniques [31], [32], MILP handles both continuous and discrete variables. In this scheme, variables, such as the status of circuit breakers are constrained to binary values (0 or 1), representing their ON or OFF states [33]. This binary decision process makes MILP highly suitable for load shedding applicationss, where circuit breakers (CBs) either disconnect or remain connected depending on the system's condition [34]. The primary objective of this scheme is to minimize the disruption to system reliability while ensuring the DC bus voltage stays within acceptable limits. The MILP algorithm allows the system to determine the amount and order of load shedding in response to varying conditions, balancing system stability and optimal load management.

B. PROBLEM FORMULATION

The optimization problem is defined by considering a microgrid connected to a total number of n of loads, consisting both critical and non-critical loads, connected to the microgrid through CBs. Non-critical loads CBs can be switched off when power demand exceeds the available supply, while critical loads remain always connected. The loads are represented by $L_1, L_2, \ldots, L_n$.

The total load connected to the microgrid at any moment is the sum of all individual loads is given as:

$$L_T = L_1 + L_2 + \ldots + L_n. \tag{1}$$

The system's total load must not exceed microgrid capacity for stable operation. This is expressed by the power constraint, given as:

$$P_{\min} \leq L_T \leq P_{\max} \tag{2}$$

where $P_{\min}$ (700 kW) represent the minimum power requirement for critical loads and $P_{\max}$ (1180 kW) represents the microgrid's maximum power supply. The constraint (2) ensures critical loads are always powered, and the total load never exceeds the available power. Furthermore, the total loads cannot exceed the maximum capacity of the supplied power $P_{\max}$ from the DERs. The upper limit $P_{\max}$ corresponds to the total capacity of the microgrid before any

event. while $P_{\min}$ is determined by the size of the critical loads, which cannot be shed at any given time. Therefore, if m denotes the number of non-critical loads that can be shed, then the non-shedable critical loads are denoted L_{CL}.

Let $x_1,\ x_2,\ \ldots\ x_m$ represent the state of the CBs attached to the non-critical loads in various areas in the microgrid, and each variable can take either 0 to indicate an OFF-state or 1 to indicate ON-state, implying, the states can only take integer values 0 and 1. Therefore, at any given time, the total number of loads connected to the network can be expressed in terms of the CBs state variables as

$$L_T = x_1L_1 + x_2L_2 + \ldots + x_mL_m + \ x_{CL}L_{CL} \tag{3}$$

where X_{CL} and L_{CL} are the circuit breaker and the load of the critical loads.

It is important to highlight the difference between Equation (1) and Equation (3). While Equation (1) represents a straightforward summation of all connected loads, Equation (3) incorporates control variables x_i (where $i = 1, 2, \ldots, m$) to enable the selective disconnection of non-critical loads. This approach facilitates optimized load shedding while ensuring that critical loads remain unaffected.

C. OBJECTIVE FUNCTION AND OPTIMIZATION

The objective function for the load-shedding problem is to maximize the connected load while maintaining system stability. Let the objective function be denoted as J, then the optimization problem can be defined as $J = L_T$.

It's important to note that the critical load circuit breaker always stays switched on. This means it's a constant value that doesn't impact the outcome of the optimization problem, [35]. As a result, we can simplify the problem significantly by rewriting the objective function based only on non-critical loads and circuit breakers (CBs).

$$J = x_1L_1 + x_2L_2 + \ldots + x_mL_m. \tag{4}$$

This objective function represents the total non-critical load that should remain connected, while critical loads are always connected and do not impact the optimization. The decision-making process is constrained by the system's power limits. The power constraint for determining CB states of non-critical loads is expressed as:

$$\mathbf{L}^T\mathbf{x} \le \mathbf{P}_{\text{con,max}} \tag{5}$$

$$-\mathbf{L}^T\mathbf{x} \le -\mathbf{P}_{\text{con,min}} \tag{6}$$

in which

$$\mathbf{x} = \begin{bmatrix} x_1 \\ x_2 \\ \vdots \\ x_m \end{bmatrix},\ \mathbf{L} = \begin{bmatrix} L_1 \\ L_2 \\ \vdots \\ L_m \end{bmatrix},$$

$$\mathbf{P}_{\text{con,max}} = P_{\max} - L_{n-m}$$

$$\mathbf{P}_{\text{con,min}} = P_{\min}$$

Also, $(\cdot)^T$ represent the transpose of vector $(\cdot)$. Considering the objective function in (4) and the power constraints in (5) and (6), The overall MILP formulation for solving the load-shedding problem is:

$$\max_{x_1,x_2,\ldots,x_m} J$$

$$\text{subject to} : \mathbf{x} \in \{0, 1\}^m,$$

$$\begin{bmatrix} \mathbf{L}^T \\ -\mathbf{L}^T \end{bmatrix}\mathbf{x} \le \begin{bmatrix} \mathbf{P}_{\max} \\ -\mathbf{P}_{\min} \end{bmatrix} \tag{7}$$

In the simulation, the maximisation problem can be converted to a minimisation problem by negating the objective function for ease of solving.

The load-shedding scheme primarily depends on voltage regulation. While the voltage is well-regulated in the grid-connected mode, it behaves differently in the islanded mode. In islanded mode, the BESS maintains power balance and regulates the DC bus voltages. As a result, this study considers the acceptable operating voltage constraint of 720V to 780V as in [20]. A voltage threshold of 720V is utilised to initiate load shedding in the large microgrid with long lines. This addresses voltage drops across the lines, which could result in significant bus deviation. Consequently, for all three categories of non-critical loads, the voltage threshold (V_{th}) is set at 720V, though this value can be increased for microgrids with shorter lines. The MILP algorithm is employed to compute the power imbalance within the system, considering the available microgrid power and the critical loads as shown in (7).

When the measured DC bus voltage V_{dc} drops below the 720V threshold and the condition persists for T_d, the MILP algorithm solves the optimisation problem to determine the optimal combination of non-critical loads to shed based on

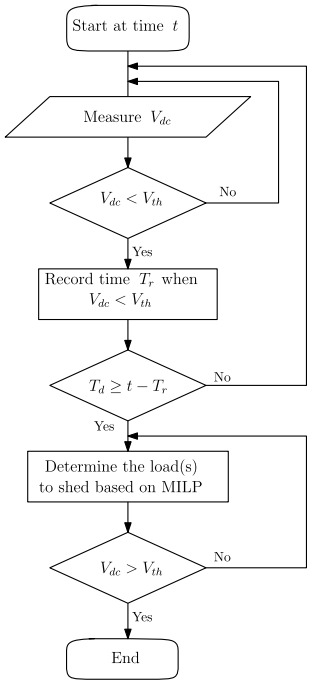

FIGURE 1. Flowchart of MILP load shedding scheme.

the detected power imbalance as shown in (7). it is worth noting that In islanded mode, the battery energy system maintains power balance and regulates DC bus voltage.

The flowchart for the proposed scheme is presented in Fig. 1, and the key steps of the algorithm are given below;

- V_{dc} is measured and compared with the voltage threshold V_{th}
- The timer mechanism ensures that the system does not shed loads prematurely. T_d represents the time delay, t is the current time, and Tr is the time of disturbance.
- The timer continuously monitors V_{dc}; when the voltage drops below V_{th} and the time difference between the current time and the time of disturbance exceeds the delay timer, the load-shedding process is initiated.
- The MILP problem is formulated and solved as soon as the shedding process is initiated to determine the non critical loads to shed.
- This continues until V_{dc} becomes greater than V_{th}

The MILP solver continues to find loads that can be shed every 10 ms based on the power imbalance between the available power and the loads until the network's V_{dc} reaches a value above the threshold voltage, V_{th}. Therefore, non-critical loads will be shed based on the magnitude of the imbalance. Three case studies will be examined: small disturbances, large disturbances, and transition from grid-connected to islanded mode to evaluate the effectiveness of the load shedding scheme.

III. DESIGN MODEL OF THE SYSTEM

The system considered for implementing the proposed load shedding scheme is the low voltage direct current (LVDC) microgrid shown in Fig 2. The system is essentially an IEEE 37-bus AC test system [8] reconfigured as a 750 V DC microgrid [36]. The IEEE 37-node feeder offers several advantages for implementing load-shedding schemes. Its realistic representation, standardization, scalability, validation and verification opportunities, and educational value make it a valuable tool for studying and improving load-shedding strategies in distribution systems [37].

The test system comprises two photovoltaic (PV) systems, two battery energy storage systems (BESS), a wind turbine (WT), and various loads. The loads considered include constant power loads C_{PL}, constant resistance loads C_{RL}, and constant current loads C_{CL}. The microgrid is interfaced with the utility using a grid-tie converter (GTC). The shaded areas in Fig. 2 indicate the three groups of noncritical loads that can be shed by tripping the corresponding fast-acting circuit breakers 1-3. The CB1, CB2, and CB3 are connected to the non-critical loads and have a total sheddable load of 200 kW, 178.5 kW, and 152.5 kW, respectively. In this study, it's important to note that there are significant voltage drops across the lines. Due to this, we have set a high load-shedding voltage threshold of 720 V for all non-critical loads to avoid over-shedding during normal operation. Additionally,

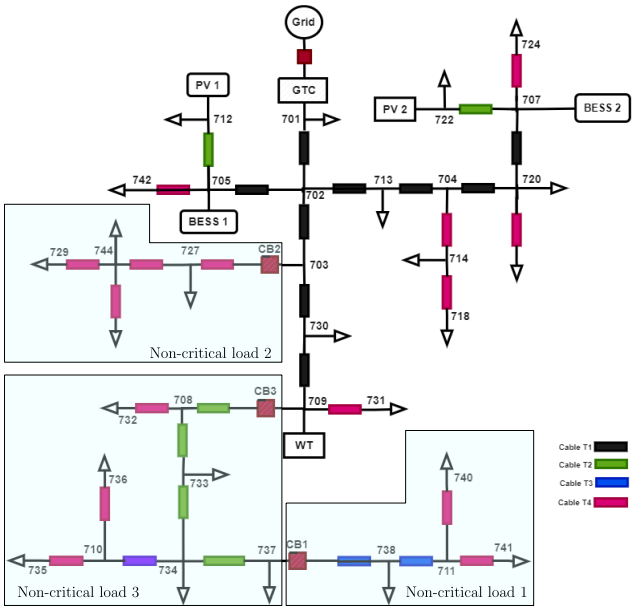

FIGURE 2. 37 Bus DC Microgrid derived from IEEE 37 Bus AC model [8].

TABLE 1. DC microgrid electrical parameters.

GTC	$S_T ransformer$ = 1 MVA	Transformer: 0.75 kV/4.8 kV
	SGTC = 1 MVA	C_{dc} = 20 mF
	V_{rated} =750 VDC	F_{sw} = 2.7 kHz
WT	P_{WT} = 1 MW	V_{rated} = 690 V
	S_{PMSG} = 1.1 MVA	C_{dc} = 20 mF
PV	P_{PV} = 5 x 0.1 MW	Max Irradiation= 1000 w/^m2
	V_{OC} = 950.5 V	I_{SC} = 714 A
	C_{dc} = 10 mF	F_{sw}= 2.7 kHz
BESS	P_{BESS} = 2×0.5 MW	V_{rated} = 700 V
	Capacity = 580Ah	C_{dc}= 10 mf
Load	Total Load	P_{load} = 1308 kW
	Non-Critical	P_{NCLoad} = 553 kW
	Critical	P_{cLoad} = 750 kW

the lowest threshold is for bus voltages over 690 V. The microgrid has a total load of 1170 kW, and the distribution line parameters vary based on the distance from the loads. In the system model, node 702 is positioned at the centre of the microgrid and is nearest to the critical loads. Therefore, it plays a vital role in evaluating the performance of all load-shedding schemes. The voltage at node 702 will be considered the reference voltage for the critical loads. A more detailed description, including the parameters of the individual loads, lines, and converter controllers, is provided in [20] and [24]. This DC microgrid network is implemented in the Matlab/Simulink environment.

IV. RESULTS OF THE PROPOSED METHOD

The islanded DC microgrid is in a steady state, where the power generated by the PV system is zero, and the WT generates 1 MW of power in the maximum power point tracking mode. At time 0.5 s, disturbances will be introduced into the system. These disturbances are caused by the gradual power reduction of WT, leading to reduced power generation.

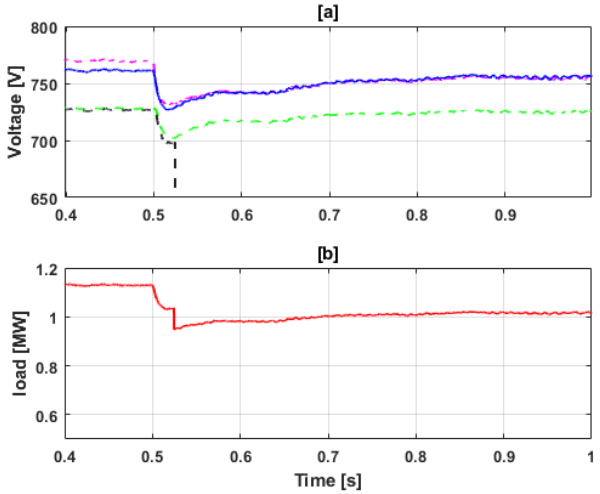

FIGURE 3. Case study 1: Performance of Adaptive scheme on small disturbance; a) DC Voltage measured at CB1, CB2, CB3 b) Load power.

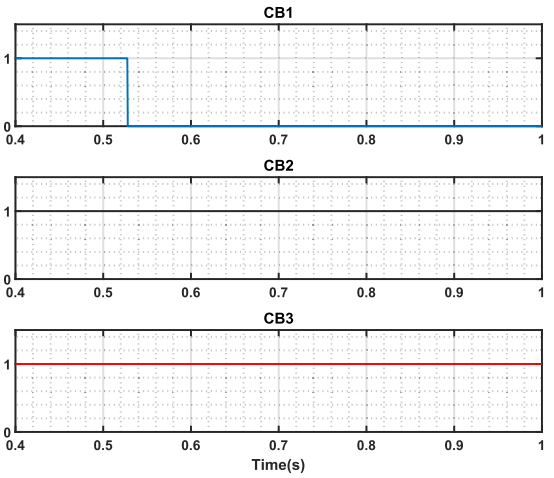

FIGURE 4. Case study 1: Circuit breakers states of the non-critical loads under adaptive timer scheme.

In such cases, load shedding is necessary. The loads are tripped based on the magnitude of the power imbalance observed by the system. Three case studies are described in the following subsections. These case studies evaluate the performance of the adaptive strategy and the proposed MILP timer-based scheme. The following metrics are used to evaluate and compare the performance of the proposed scheme:

- Response Time: The time taken for circuit breakers to trip following a disturbance.
- Voltage Stabilization: The scheme's ability to maintain the voltage within a specified range is measured by the minimum voltage of critical loads during a disturbance and the final voltage after the disturbance is resolved.
- Load-Shedding Efficiency: Assessed by the extent to which unnecessary load shedding is prevented and the precision in shedding non-critical loads proportional to the magnitude of the disturbance.

The DC microgrid network was simulated using a sampling of 5μs. The MILP was solved using the `intlinprog` function in MATLAB, with computation times typically found to be less than $2-3\mu$s, indicating the suitability of the method for online applications.

A. CASE STUDY 1: SMALL DISTURBANCE

This case study examines the performance of a proposed scheme under small disturbances (200 kW). Initially, the wind turbine generated 700 kW of power in MPPT mode, but the PV units were not operational. The loads consumed 1.18 MW, and the voltages ranged from 720 V to 780 V. Due to changes in wind speed, the wind turbine's power generation declined gradually from 700 kW to 500 kW in 0.5 seconds, causing a decrease in microgrid bus voltages. A comparison was made between the performance of the adaptive timer scheme [24]

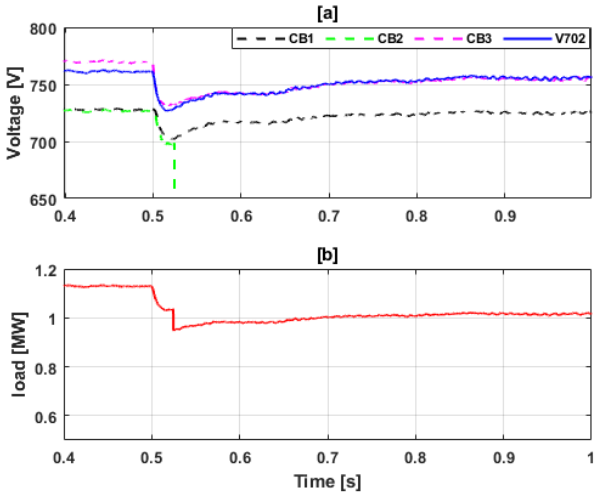

FIGURE 5. Case study 1: Performance of MILP Scheme on small disturbance; a) DC Voltage measured at CB1, CB2, CB3 b) Load power.

and the proposed MILP timer-based scheme. In the MILP timer-based scheme, a time delay of $T_d = 20$ ms was utilized to enable the system to process any disturbances. In contrast, the adaptive scheme maintained a time delay of 15 ms, as reported in [24].

1) ADAPTIVE SCHEME

Figure 3 illustrates the voltage and power during a small disturbance. At the time $t = 0.528$ seconds, the system responded by tripping CB1 with a load of 200 kW as shown in Fig. 4, because the voltage had fallen below the threshold of 720 V to 719 V. CB1 has shed loads and the voltage of the critical loads was regulated at 750 V, as shown in fig 3a. After shedding, the microgrid's load was maintained at 980 kW, as shown in fig 3b.

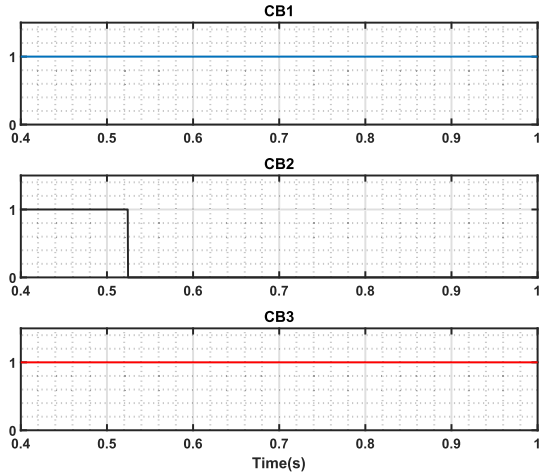

FIGURE 6. Case study 1: Circuit breakers states of the non-critical loads under MILP scheme.

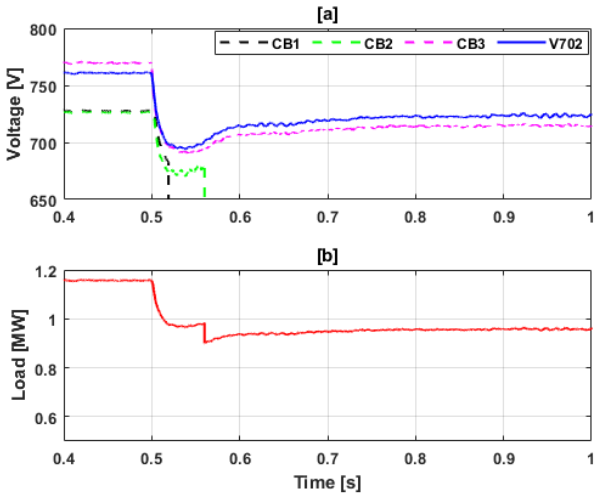

FIGURE 7. Case 2: Circuit breakers states of the non-critical loads under adaptive scheme.

2) PROPOSED MILP TIMER-BASED SCHEME

Fig. 5 illustrates the performance of the proposed MILP timer-based scheme during a small disturbance. As shown in Fig. 6, non-critical loads were shed by tripping CB2 with a load of 178 kW at $t = 0.524$ seconds. CB2 tripped when the voltage dropped below 720 V to 719 V. The voltage was then regulated at 750 V after shedding. Fig. 5b illustrates the responses of the total load power 1180 kW before disturbance and after the circuit breakers were tripped at 1.002 kW.

According to the results, the MILP timer-based scheme shed non-critical loads slightly faster than the adaptive scheme. The proposed scheme has tripped CB2, which has a total non-critical load of 178 kW. On the other hand, the adaptive scheme tripped CB1, which has a non-critical load of 200 kW. This shows that the MILP timer-based scheme is capable of shedding loads of the same magnitude as the disturbance observed.

B. CASE STUDY 2: LARGE DISTURBANCE

This case study focuses on the performance analysis of the adaptive timer-based scheme and the MILP timer-based scheme when exposed to a large disturbance. Before the disturbance, the DC microgrid operated in a stable state with faulty PV generation. The wind turbine generated 1 MW of power while operating in MPPT mode. The total power demand was 1.18 MW, and two BESSs regulated the DC bus voltages, each providing 0.27 MW of power and maintaining the voltage levels between 720V and 770V.

At time t=0.5s, an internal fault caused the wind turbine to disconnect from the microgrid. As a result, each (BESS) outputted a maximum of 0.41 MW, which was not enough to sustain the system's stability. Consequently, the voltage on the bus decreased significantly, leading to further instability in the system.

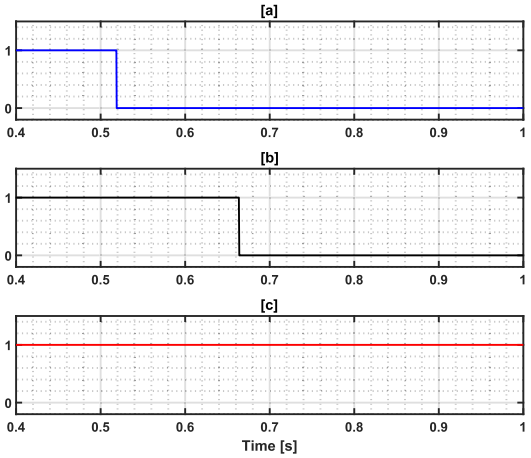

FIGURE 8. Case 2: Circuit breakers states of the non-critical loads under MILP scheme.

1) ADAPTIVE TIMER-BASED SCHEME

Fig. 7 illustrates how the voltage and power behaved when an adaptive timer-based scheme was employed. The CB1 and CB2 were tripped at $t = 0.519$ s and $t = 0.56$ s, respectively, in response to laying off a load of 378.5 KW as shown in Fig. 8. Due to the magnitude of the ROCOV, CB1 reacted quickly. CB3 was not tripped since ROCOV became positive after shedding CB1 and CB2 as explained in [25]. As a result, the voltage for the critical loads went down to 690 V, close to the lowest threshold of 680 V. The voltage of the critical loads was regulated and maintained at 720 V after 0.25 s of the disturbance, as shown in Fig. 7a. The total load in the system after CB1 and CB2 were tripped was 0.91 MW, as illustrated in Fig. 7b

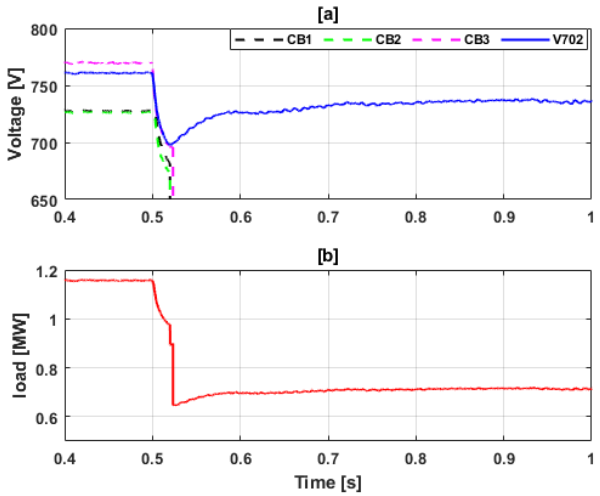

FIGURE 9. Case 2: Performance of Adaptive Scheme; a) DC Voltage measured at CB1, CB2, CB3 b) Load power.

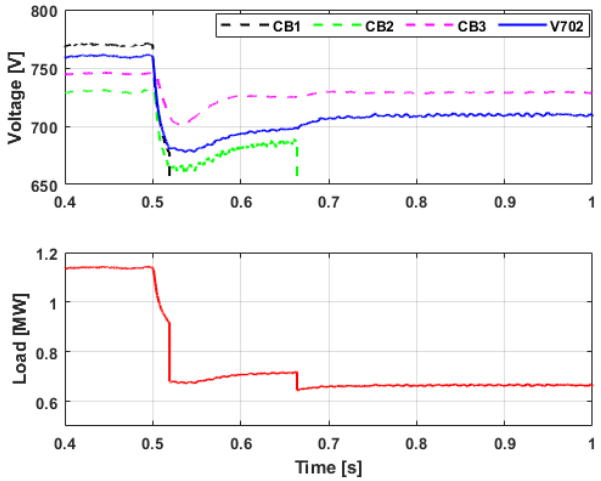

FIGURE 11. Case 3: Performance of MILP Scheme; a) DC Voltage measured at CB1, CB2, CB3 b) Load power.

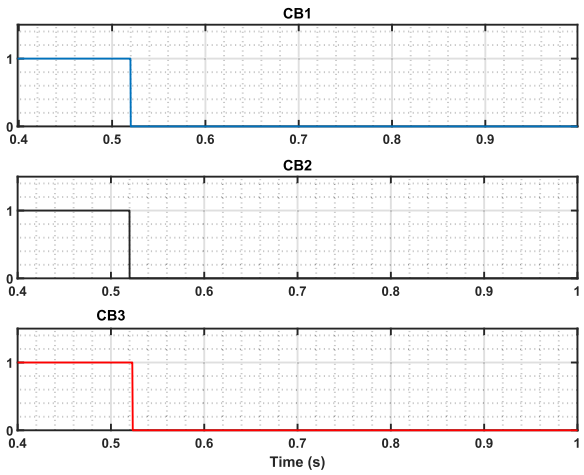

FIGURE 10. Case 2: Circuit breakers states of the non-critical loads under adaptive scheme.

2) PROPOSED MILP TIMER-BASED SCHEME

Fig. 9 illustrates how the proposed MILP timer-based scheme responds to a significant disturbance. At $t = 0.52$ s, CB2 with a load of 178.5 KW trips to shed non-critical loads in area 2. CB1 with a load of 200 KW and CB3 with a load of 152.5 were tripped simultaneously at $t = 0.5234$ s. As a result, the voltage of the critical loads did not drop below 690 V and returned to 740 V within 0.20 s after the disturbance hit the system, as shown in Fig. 9a. This proves the proposed MILP timer-based scheme responds quicker than the adaptive schemes. All non-critical loads were shed within a period of 3.4 ms at the occurrence of the disturbance, as shown in Fig. 10. After CB1, CB2, and CB3 tripped, the total load in the system became 0.72 MW, as shown in Fig. 9b

C. CASE STUDY 3: ISLANDED EVENT

This case study examines the performances of adaptive and MILP timer-based strategies after an islanding event. At $t < 0.5$ s, the microgrid is grid-connected.The wind turbine generates 0.20 MW of power. However, the PV units do not produce any power at night. The BESSs provide 0.16 MW of power, while the power demand in the microgrid is 1.18 MW. The GTC imports 0.88 MW from the utility grid to maintain power balance. The GTC also ensures that the DC bus voltages remain between 720 V and 770 V.

Due to an unintentional islanding event at $t = 0.5$ s, the GTC stops importing power with the host utility grid. To react to this disturbance, each BESS provides its rated power of 0.410 MW to the islanded microgrid. However, this power is not enough to meet the power demand in the islanded system; they will fall immediately. The performance of the subsequent adaptive timer strategy and the proposed MILP timer-based strategy is presented below.

1) ADAPTIVE TIMER BASED SCHEME

The adaptive timer strategy sheds non-critical loads on CB1 and CB2 with total loads of 378.5 KW at 0.52 s and 0.667 s, respectively. The CB1 tripped fast due to the high magnitude of ROCOV, while CB2 took longer to shed due to the time delay used. This resulted in a voltage sag, but the critical load voltage remained above 690 V. CB3 did not trip due to the ROCOV being positive, and the voltage of the critical loads was restored to 705 volts within 0.15 seconds, as shown in Fig. 11 and 12.

2) PROPOSED MILP TIMER BASED

The proposed MILP load-shedding scheme sheds non-critical loads on CB2 and CB3 at time 0.52 s, as shown in Fig. 14. This reduces the total load power demand to 925 kW, and the critical load voltage is regulated to an acceptable level of 720 V within approximately 0.25 s after the disturbance shown in Fig. 13.

Based on the results of three case studies, the proposed MILP timer-based schemes have shown to perform better

TABLE 2. Summary of comparison of MILP and adaptive timer based schemes.

Disturbance	LS Scheme	Trip Time CB1 (s)	Trip Time CB2 (s)	Trip Time CB3 (s)	Vmin (V)	Vfinal (V)
Small	Proposed Scheme	0	0.524	0	719	750
	Adaptive Timer	0.528	0	0	719	750
Large	Proposed Scheme	0.52	0.52	0.523	695	740
	Adaptive Timer	0.519	0.56	0	690	720
Islanded	Proposed Scheme	0	0.52	0.52	691	720
	Adaptive Timer	0.52	0.667	0	695	705

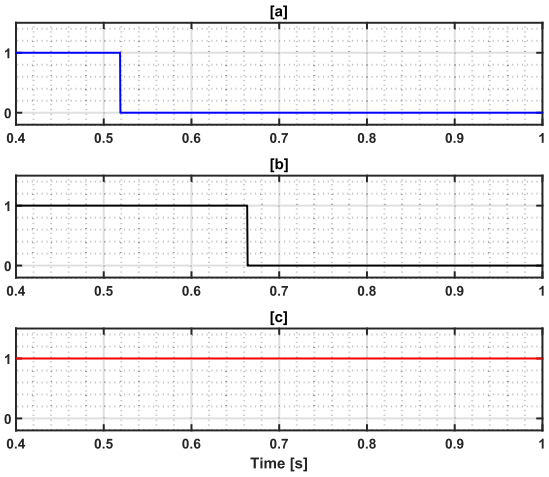

FIGURE 12. Case 3: Circuit breakers states of the non-critical loads under MILP scheme.

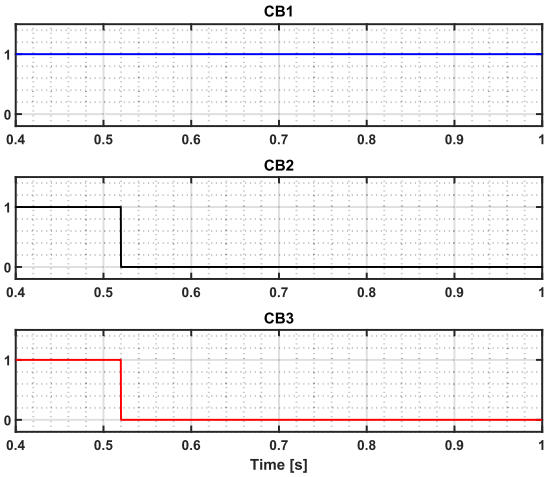

FIGURE 14. Case 3: Circuit breakers states of the non-critical loads under MILP scheme.

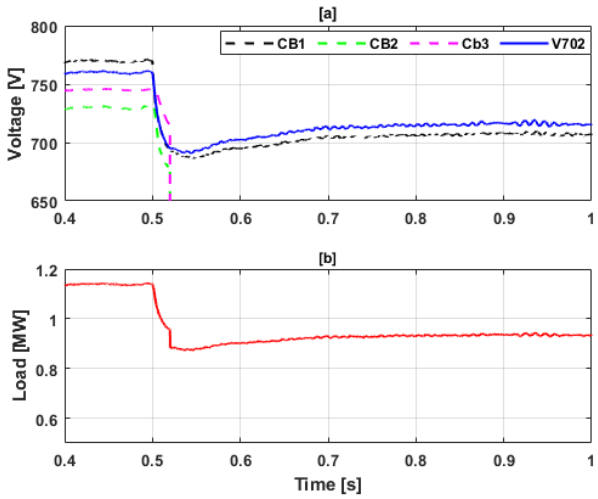

FIGURE 13. Case 3: Performance of MILP Scheme; a) DC Voltage measured at CB1, CB2, CB3 b) Load power.

regarding the speed (time) of shedding and the number of loads to shed in different disturbances, as shown in 2. Some of the advantages of the proposed MILP timer-based scheme over adaptive schemes can be summarized as follows:

- The adaptive scheme requires a predetermined CB1, CB2, and CB3 sequence to activate the breakers when disturbances occur. On the other hand, the proposed MILP timer-based scheme trips the circuit breakers based on the magnitude of the detected disturbance without following any specific sequence. This approach enables the proposed scheme to shed the best combination of loads for optimal operation and reliability of the microgrid.
- The adaptive scheme results shown in Fig. 7 and in Fig. 11 regulate the system voltage at lower voltages, which could expose critical loads to lower voltages after load shedding. On the other hand, the proposed MILP timer-based scheme regulates the system voltage at higher voltages due to its faster response to any disturbance, as depicted in Fig. 9 and Fig. 13.
- The proposed technique can measure and predict power imbalance more accurately than the adaptive scheme. This is because it does not involve a derivative (dv/dt) component, sometimes slowing CBs' response by approximating voltage measurement.

Table 2 summarizes the results of three case studies, comparing the performance metrics of an adaptive timer-based scheme with that of the proposed MILP timer-based scheme. The table displays the trip time of the circuit breakers, the minimum voltage experienced V_{min}, and the final regulated voltage V_{final} shared by the critical loads.

V. CONCLUSION

This paper presents a novel MILP timer-based load-shedding scheme for islanded DC microgrids, addressing key challenges associated with conventional and adaptive load-shedding techniques. The proposed strategy integrates

a short delay mechanism with a Mixed Integer Linear Programming (MILP) algorithm to optimize load-shedding decisions. By leveraging local voltage measurements, the scheme dynamically determines the optimal amount of non-critical loads to shed, ensuring faster, more precise, and proportional load-shedding actions. Simulation results on a DC microgrid model adapted from the IEEE 37-bus network demonstrate the scheme's effectiveness in improving system performance. The proposed method achieves a 25% faster response time for shedding non-critical loads compared to adaptive timer-based schemes, significantly reducing recovery time during disturbances. Additionally, it minimizes voltage sags by up to 18%, ensuring that the DC bus voltage consistently remains above the critical threshold of 720 V, thereby safeguarding critical loads from exposure to low voltage conditions. The strategy also reduces over-shedding events by 20%, enhancing system reliability and minimizing unnecessary load disconnections. The ability to coordinate multiple load-shedding steps, proportional to the magnitude of the disturbance, addresses the shortcomings of traditional step-by-step approaches. By optimizing the load-shedding process, the proposed scheme mitigates the risks of over-shedding, reduces voltage deviations, and maintains power balance during severe disturbances. Furthermore, the proposed method offers a scalable and robust solution suitable for large DC microgrids with diverse load configurations and multiple circuit breakers. These advancements highlight the potential of the MILP timer-based load-shedding scheme to significantly improve the stability, reliability, and resilience of islanded DC microgrids. The approach offers a practical, communication-independent solution for modern DC microgrids, ensuring enhanced operational efficiency and robustness during disturbances.

FUTURE WORK

The research described in this paper sets the stage for future studies on more advanced DC load-shedding strategies. To build on this work, future research could involve testing the approach on actual hardware to ensure its practicality and performance in real microgrid settings. Additionally, the model could be enhanced by incorporating nonlinear characteristics and using Nonlinear Programming (NLP) or MINLP to better represent the system's behaviour. Another interesting area for future investigation is the coordination of significantly larger networks, where the number of circuit breakers (CBs) to be managed increases substantially.

REFERENCES

[1] J. Namaganda-Kiyimba and J. Mutale, "An optimal rural community PV microgrid design using mixed integer linear programming and DBSCAN approach," *SAIEE Afr. Res. J.*, vol. 111, no. 3, pp. 111–119, Sep. 2020.

[2] M. Shamsoddini, B. Vahidi, R. Razani, and Y. A.-R.-I. Mohamed, "A novel protection scheme for low voltage DC microgrid using inductance estimation," *Int. J. Electr. Power Energy Syst.*, vol. 120, Sep. 2020, Art. no. 105992.

[3] J. P. Murenzi and T. S. Ustun, "The case for microgrids in electrifying Sub–Saharan Africa," in *Proc. 6th Int. Renew. Energy Congr. (IREC)*, Mar. 2015, pp. 1–6.

[4] Y. B. Aemro, P. Moura, and A. T. de Almeida, "Design and modeling of a standalone DC-microgrid for off-grid schools in rural areas of developing countries," *Energies*, vol. 13, no. 23, p. 6379, Dec. 2020.

[5] W. Feng, M. Jin, X. Liu, Y. Bao, C. Marnay, C. Yao, and J. Yu, "A review of microgrid development in the United States—A decade of progress on policies, demonstrations, controls, and software tools," *Appl. Energy*, vol. 228, pp. 1656–1668, Oct. 2018.

[6] P. Pan and R. K. Mandal, "Fault detection and classification in DC microgrid clusters," *Eng. Res. Exp.*, vol. 5, no. 2, Jun. 2023, Art. no. 025010.

[7] E. Planas, J. Andreu, J. I. Gárate, I. Martínez de Alegría, and E. Ibarra, "AC and DC technology in microgrids: A review," *Renew. Sustain. Energy Rev.*, vol. 43, pp. 726–749, Dec. 2014.

[8] R. Ziesche, T. M. M. Heenan, P. Kumari, J. Williams, W. Li, M. E. Curd, T. L. Burnett, I. Robinson, D. J. L. Brett, M. J. Ehrhardt, P. D. Quinn, B. L. Mehdi, P. J. Withers, M. M. Britton, N. D. Browning, and P. R. Shearing, "Multi-dimensional characterization of battery materials," *Adv. Energy Mater.*, vol. 13, no. 23, May 2023, Art. no. 2300103.

[9] E. Hossain, E. Kabalci, R. Bayindir, and R. Perez, "Microgrid testbeds around the world: State of art," *Energy Convers. Manage.*, vol. 86, pp. 132–153, Oct. 2014.

[10] P. Sanjeev, N. P. Padhy, and P. Agarwal, "Autonomous power control and management between standalone DC microgrids," *IEEE Trans. Ind. Informat.*, vol. 14, no. 7, pp. 2941–2950, Jul. 2018.

[11] H. H. Coban, A. Rehman, and M. Mousa, "Load frequency control of microgrid system by battery and pumped-hydro energy storage," *Water*, vol. 14, no. 11, p. 1818, Jun. 2022.

[12] Y. Xia, M. Yu, P. Yang, Y. Peng, and W. Wei, "Generation-storage coordination for islanded DC microgrids dominated by PV generators," *IEEE Trans. Energy Convers.*, vol. 34, no. 1, pp. 130–138, Mar. 2019.

[13] L. Yan, M. Sheikholeslami, W. Gong, M. Shahidehpour, and Z. Li, "Architecture, control, and implementation of networked microgrids for future distribution systems," *J. Modern Power Syst. Clean Energy*, vol. 10, no. 2, pp. 286–299, Mar. 2022.

[14] P. Yang, M. Yu, Q. Wu, N. Hatziargyriou, Y. Xia, and W. Wei, "Decentralized bidirectional voltage supporting control for multi-mode hybrid AC/DC microgrid," *IEEE Trans. Smart Grid*, vol. 11, no. 3, pp. 2615–2626, May 2020.

[15] S. Sahoo and S. Mishra, "A multi-objective adaptive control framework in autonomous DC microgrid," *IEEE Trans. Smart Grid*, vol. 9, no. 5, pp. 4918–4929, Sep. 2018.

[16] N. N. A. Bakar, M. Y. Hassan, M. F. Sulaima, M. N. M. Nasir, and A. Khamis, "Microgrid and load shedding scheme during islanded mode: A review," *Renew. Sustain. Energy Rev.*, vol. 71, pp. 161–169, May 2017.

[17] N. M. Sapari, H. Mokhlis, J. A. Laghari, A. H. A. Bakar, and M. R. M. Dahalan, "Application of load shedding schemes for distribution network connected with distributed generation: A review," *Renew. Sustain. Energy Rev.*, vol. 82, pp. 858–867, Feb. 2018.

[18] J. Meng, Y. Wang, C. Wang, and H. Wang, "Design and implementation of hardware-in-the-loop simulation system for testing control and operation of DC microgrid with multiple distributed generation units," *IET Gener., Transmiss. Distrib.*, vol. 11, no. 12, pp. 3065–3072, Aug. 2017.

[19] L. Gao, Y. Liu, H. Ren, and J. Guerrero, "A DC microgrid coordinated control strategy based on integrator current-sharing," *Energies*, vol. 10, no. 8, p. 1116, Aug. 2017. [Online]. Available: https://www.mdpi.com/1996-1073/10/8/1116

[20] A. Babagana, T. Zaman, Y. Seferi, M. Syed, and G. Burt, "Comparison of non-communication based DC load shedding schemes," in *Proc. 57th Int. Universities Power Eng. Conf. (UPEC)*, Aug. 2022, pp. 1–6.

[21] J. Mohammadi and F. B. Ajaei, "DC microgrid load shedding schemes," in *Proc. IEEE/IAS 55th Ind. Commercial Power Syst. Tech. Conf. (I&CPS)*, May 2019, pp. 1–7.

[22] D. Chen, L. Xu, and L. Yao, "DC voltage variation based autonomous control of DC microgrids," *IEEE Trans. Power Del.*, vol. 28, no. 2, pp. 637–648, Apr. 2013.

[23] J. Mohammadi and F. B. Ajaei, "Adaptive time delay strategy for reliable load shedding in the direct-current microgrid," *IEEE Access*, vol. 8, pp. 114509–114518, 2020.

[24] J. Mohammadi and F. B. Ajaei, "Adaptive voltage-based load shedding scheme for the DC microgrid," *IEEE Access*, vol. 7, pp. 106002–106010, 2019.

[25] F. Zare, H. K. Kargar, and A. Salemnia, "An improved priority-based load shedding scheme in hybrid AC/DC microgrids using micro-PMUData," in *Proc. 28th Iranian Conf. Electr. Eng. (ICEE)*, Aug. 2020, pp. 1–5.
[26] R. Hooshmand and M. Moazzami, "Optimal design of adaptive under frequency load shedding using artificial neural networks in isolated power system," *Int. J. Electr. Power Energy Syst.*, vol. 42, no. 1, pp. 220–228, Nov. 2012.
[27] S. Sundarajoo and D. M. Soomro, "Optimal load shedding for voltage collapse prevention following overloads in distribution system," *Int. J. Eng.*, vol. 36, no. 7, pp. 1230–1238, 2023.
[28] W. P. Luan, M. R. Irving, and J. S. Daniel, "Genetic algorithm for supply restoration and optimal load shedding in power system distribution networks," *IEEE Proc. Gener., Transmiss. Distrib.*, vol. 149, no. 2, pp. 145–151, Mar. 2002.
[29] M. J. Aliabadi and M. Radmehr, "Hybrid energy system optimization integrated with battery storage in radial distribution networks considering reliability and a robust framework," *Sci. Rep.*, vol. 14, no. 1, p. 26597, 2024.
[30] H. Dai, G. Huang, J. Wang, and H. Zeng, "VAR-tree model based spatio-temporal characterization and prediction of O3 concentration in China," *Ecotoxicol. Environ. Saf.*, vol. 257, Jun. 2023, Art. no. 114960.
[31] V. Skiparev, K. Nosrati, A. Tepljakov, E. Petlenkov, Y. Levron, J. Belikov, and J. M. Guerrero, "Virtual inertia control of isolated microgrids using an NN-based VFOPID controller," *IEEE Trans. Sustain. Energy*, vol. 14, no. 3, pp. 1558–1568, Jan. 2023.
[32] S. Sarwar, H. Mokhlis, M. Othman, M. A. Muhammad, J. A. Laghari, N. N. Mansor, H. Mohamad, and A. Pourdaryaei, "A mixed integer linear programming based load shedding technique for improving the sustainability of islanded distribution systems," *Sustainability*, vol. 12, no. 15, p. 6234, Aug. 2020.
[33] L. Weimann, P. Gabrielli, A. Boldrini, G. J. Kramer, and M. Gazzani, "On the role of H_2 storage and conversion for wind power production in The Netherlands," in *Computer Aided Chemical Engineering*, vol. 46. Amsterdam, The Netherlands: Elsevier, 2019, pp. 1627–1632.
[34] P. Pourghasem, H. Seyedi, and K. Zare, "A new optimal under-voltage load shedding scheme for voltage collapse prevention in a multi-microgrid system," *Electric Power Syst. Res.*, vol. 203, Feb. 2022, Art. no. 107629.
[35] G. S. Thirunavukkarasu, M. Seyedmahmoudian, E. Jamei, B. Horan, S. Mekhilef, and A. Stojcevski, "Role of optimization techniques in microgrid energy management systems—A review," *Energy Strategy Rev.*, vol. 43, Sep. 2022, Art. no. 100899.
[36] L. Xu and D. Chen, "Control and operation of a DC microgrid with variable generation and energy storage," *IEEE Trans. Power Del.*, vol. 26, no. 4, pp. 2513–2522, Oct. 2011.
[37] D. Sarajlic and C. Rehtanz, "Overview of distribution grid test systems for benchmarking of power system analyses," in *Proc. AEIT Int. Annu. Conf.*, Sep. 2020, pp. 1–6.

ABDULRAHMAN BABAGANA (Student Member, IEEE) received the B.Eng. degree in electrical and electronic engineering from the University of Maiduguri, in 2008, and the M.Sc. degree in applied instrumentation and control from Glasgow Caledonian University, in 2012. He is currently pursuing the Ph.D. degree in electronics and electrical engineering with the University of Strathclyde, Glasgow, U.K. Before starting the Ph.D. degree, in June 2020, he was a Lecturer with the University of Maiduguri. His research interests include DC systems, power system instrumentation, protection, disturbance identification, resiliency, and control.

ISAH A. JIMOH (Student Member, IEEE) received the B.Eng. degree in electrical and electronic engineering from the University of Benin and the M.Sc. degree in applied instrumentation and control from Glasgow Caledonian University, in 2016 and 2018, respectively. He is currently pursuing the Ph.D. degree with the Wind Energy and Control Centre, University of Strathclyde. He investigates optimal control applications to nonlinear systems with the University of Strathclyde. His research interests include optimal control and the analysis and performance optimization of dynamic systems.

YLJON SEFERI received the M.Sc. degree in electrical engineering from the Polytechnic University of Tirana, in 2007, and the Ph.D. degree from the University of Strathclyde, in 2022. He is currently a Research Associate with the Institute of Energy and Environment, University of Strathclyde, Glasgow, Scotland. His research interests include power quality studies and metrics for AC and DC electrified railway systems, arc fault generation methods for DC distribution systems, power and energy measurements, and electrical metrology.

GRAEME BURT (Member, IEEE) received the B.Eng. degree in electrical and electronic engineering and the Ph.D. degree in fault diagnostics in power system networks from the University of Strathclyde, Glasgow, U.K., in 1988 and 1992, respectively. He is currently a Distinguished Professor in electrical power systems with the University of Strathclyde, where he directs the Institute for Energy and Environment, directs the Rolls-Royce University Technology Centre in Electrical Power Systems, and the Lead Academic for the Power Networks Demonstration Centre. He is on the board of DERlab e.V., the association of distributed energy laboratories. His research interests include the areas of decentralized energy and smart grid protection and control, electrification of aerospace and marine propulsion, DC and hybrid power distribution, and experimental systems testing and validation with power hardware in the loop.